ACS Catalysis

Research Article

Cite This: ACS Catal. 2019, 9, 4360−4368

pubs.acs.org/acscatalysis

Selective Oxidation of Acetaldehyde to Acetic Acid on Pd−Au Bimetallic Model Catalysts

Sungmin Han,[†] Kihyun Shin,[†,‡] Graeme Henkelman,[†,‡] and C. Buddie Mullins*[,†,§]

[†]Department of Chemistry, University of Texas at Austin, Austin, Texas 78712-0231, United States

[‡]Institute for Computational Engineering and Science, University of Texas at Austin, Austin, Texas 78712-0231, United States

[§]McKetta Department of Chemical Engineering, Center for Nano and Molecular Science and Technology, Texas Materials Institute, Center for Electrochemistry, University of Texas at Austin, Austin, Texas 78712-0231, United States

Supporting Information

ABSTRACT: Acetic acid is a widely employed reactant in the chemical industry, and it is also used as a food ingredient. Here, we report a catalytic reaction pathway for the gas-phase selective oxidation of acetaldehyde to acetic acid on a Pd−Au(111) heterogeneous model catalyst. On an oxygen precovered Pd−Au surface, acetaldehyde is selectively oxidized to acetic acid from 250 to 340 K. Using FT-IR, the formation of acetate species is detected from 160 to 260 K on this surface, which is a widely known adsorbate derived from acetic acid on metal surfaces. With higher Pd coverages, the acetaldehyde is less selectively oxidized to acetic acid, and near 375 K, CO_2, H_2O, CH_4, and H_2 are evolved, evidence for the decarboxylation of acetate. In our density functional theory calculations, we confirm that the relative energy difference between the acetate state and the decarboxylated state decreases as Pd ensemble size increases.

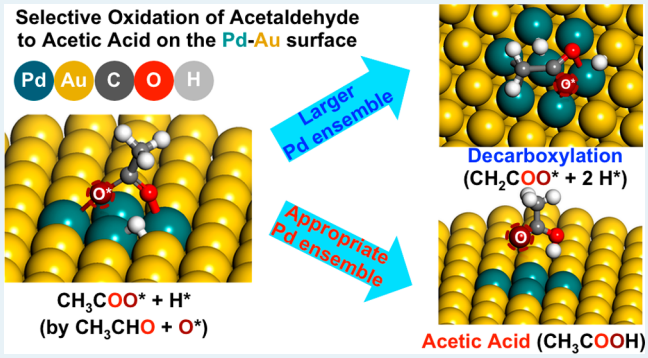

KEYWORDS: *acetaldehyde desorption, O_2 activation, acetaldehyde oxidation, acetic acid production, Pd−Au bimetallic catalyst, surface chemistry*

INTRODUCTION

Acetic acid (CH_3COOH, AcOH) is familiar as a food preservative, such as vinegar, and is produced by alcohol fermentation. AcOH is also a major reactant for synthesizing commercial chemicals such as vinyl acetate, acetic anhydride, and various esters (e.g., ethyl acetate, *n*-butyl, and isobutyl acetate).[1−3] Because of its wide use the global demand for AcOH grew from 5.4 million tons in 1997 to 13 million tons in 2015, and it is expected to reach 18 million tons in 2020.[1,2]

One of the conventional routes for manufacturing AcOH is the oxidation of acetaldehyde (CH_3CHO, AcAl) at 150 °C and 55 atm with manganese(II) or cobalt(II) acetate catalysts.[1−3] This process produces some side products, such as ethyl acetate, formic acid, and formaldehyde, although the overall yield of this process can reach 95%. After the first adaptation of the methanol carbonylation process in 1960 by BASF, most industrial synthesis of AcOH has followed the Monsanto and Cativa processes, which are the more advanced methanol carbonylation schemes.[1−3] In these operations, Rh and Ir based organometallic catalysts are used in the temperature and pressure ranges of 150−200 °C and 30−50 atm, and the selectivity toward AcOH is ∼99%.[1,2] Since all methanol carbonylation processes are solution based, distillation and separation steps are necessary for purifying the AcOH from the reaction mixture.[4] Here we report a new vapor-phase heterogeneous catalytic process for the selective oxidation of AcAl to AcOH near room temperature over Pd−Au bimetallic model catalysts which would require fewer separation steps.

Pd−Au nanoparticles have shown impressive catalytic activities in the synthesis of vinyl acetate,[5,6] H_2O_2,[7−9] the oxidation of alcohols,[10−12] and CO,[13−15] which are mainly due to the so-called ensemble effect, determined by the local compositions of Pd and Au atoms. For a better understanding of these catalytic reactions based on surface composition, the detailed molecular level chemistry has been also investigated by adopting Pd−Au model catalytic surfaces under ultrahigh vacuum (UHV). Specifically, it has been found that the distance between Pd monomers on Au surfaces is a key for the promotional effect in vinyl acetate synthesis[16] and that the Pd−Au interfaces are the reactive areas for the selective production of H_2 from the decomposition of formic acid (HCOOH).[17] The behavior of simple molecules (e.g., O_2,[18,19] H_2,[20−22] CO,[23−25] H_2O,[26] and CH_3CH_2OH[27]) on Pd−Au surfaces has also been widely studied. In particular, the H_2

Received: January 7, 2019
Revised: March 26, 2019
Published: April 9, 2019

DOI: 10.1021/acscatal.9b00079
ACS Catal. 2019, 9, 4360−4368

desorption behavior can be used to analyze the surface composition of Pd and Au. The recombinative desorption of H_2 occurs between 150 K - 300 K for Pd−Au interface sites (or discontinuous and small Pd ensembles),[17,19,21,27] which is higher than the desorption temperatures of H_2 on the pure Au(111) surface (<150 K)[28] and lower than on pure Pd surfaces (>300 K).[29,30] When the Pd coverage on the Au(111) surface becomes large enough to form Pd(111)-like islands (or sufficiently large Pd ensembles to have pure Pd-like character), there is another H_2 desorption feature above 300 K, which corresponds to the desorption of H_2 from pure Pd surfaces.[17,19,21,27] Moreover, we have experimentally verified that Pd(111)-like island sites (large enough Pd ensembles to have Pd(111)-like character) are necessary for the dissociative adsorption of O_2.[19] Furthermore, the reactivity of the dissociated oxygen adatoms depends on the concentration of Pd−Au interface sites.[19]

Motivated by these results, we now focus on the oxidation of AcAl to AcOH on Pd−Au(111) model catalysts. Previously, it has been found that oxygen adatoms placed on Au(111) [via ozone] can oxidize acetaldehyde to acetic acid from ∼460 K.[31] Although AcOH is also produced from the oxidation of AcAl on pure Pd surfaces above 400 K,[32] it is accompanied by the generation of other oxidized products (e.g., CO, CO_2, and H_2O), thereby decreasing the selectivity toward AcOH. This is primarily because the acetate species (CH_3COO*) on pure Pd surfaces, formed by oxygen adatoms (O*) and acetyl (CH_3CO*, deprotonated acetaldehyde) can be decarboxylated, which is initiated by the dissociation of β−C-H bonds in the acetate species.[32−34] However, we have found that the decarboxylation of acetate can be prevented by controlling the surface composition of Pd and Au, and it leads to the selective oxidation of AcAl to AcOH near room temperature. We have investigated the detailed chemistry using quadrupole mass spectroscopy and FT-IR spectroscopy as well as density functional theory (DFT) calculations.

EXPERIMENTAL SECTION

Ultrahigh Vacuum (UHV) Experiments. All experiments in the present study were conducted in a UHV molecular beam surface scattering system with a base pressure of 1.0×10^{-10} Torr, which has been carefully described in a previous paper.[35] In brief, the apparatus can generate two separate molecular beams, and is equipped with an Auger electron spectrometer (Physical Electronics 10−500), a quadrupole mass spectrometer (Extrel C-50), and a Fourier transform infrared spectrometer (Bruker Tensor 27) with a mercury−cadmium−telluride (MCT) detector. A disk shaped Au(111) single crystal sample (12 mm in diameter× 2 mm thickness) is held by a Mo wire fitted in a groove cut on the edge of the Au(111) sample in the UHV chamber. This Au(111) sample was periodically cleaned by Ar sputtering and then annealed to 800 K. The Mo wire is used to resistively heat the sample and also to cool the sample to 77 K by providing thermal contact with a liquid nitrogen bath. The sample temperature was measured by a K-type thermocouple placed in a small hole in the edge of the sample.

The Pd−Au model surface was prepared based on a layer by layer growth mechanism, in which the Pd atoms can diffuse into the bulk of the Au(111) sample by heating to form a Pd−Au alloy on the top surface.[36] The Pd deposition was calibrated by a quartz crystal microbalance (QCM) and controller (Maxtek Inc.) with the assumption of a thickness of 1 monolayer (ML) for Pd as 2.74 Å. In this study, two different Pd coverages (2.0 and 3.0 ML) were deposited on the Au(111) surface at 77 K and then annealed to 500 K for 10 min as with our previous studies to form a Pd−Au alloy at the surface.[17−19,26] Each of the annealed Pd−Au surfaces was also exposed to O_2 molecules at 475 K via the molecular beam to treat the surfaces with O_2 for consistency with our previous O_2 activation and reactivity study.[19]

All gas molecules were delivered via a molecular beam, which allows for the accurate control of the amount of adsorbed target molecules on the surface. Temperature-programmed desorption (TPD) was adopted in this study to analyze the surface composition of Pd−Au surfaces using H_2 and to investigate the oxidation chemistry of acetaldehyde. For the H_2-TPD, we initially saturated the Pd−Au surfaces with H_2 via a H_2 molecular beam at 77 K and then heated to 500 at 1 K/s while observing the $m/z^+ = 2$ signal with the QMS. To test the oxidation of AcAl, each Pd−Au surface was first exposed to a O_2 molecular beam at 300 K until it was saturated with oxygen adatoms, and then the surface was cooled to 77 K. AcAl molecules were then impinged on the O-precovered Pd−Au surfaces at 77 K via an AcAl molecular beam, followed by heating of the sample to 500 at 1 K/s while detecting various masses using the QMS. Heating the surfaces to 500 K did not affect their Au and Pd compositions, which has been verified in our previous studies.[18,19,26] After finishing the TPD of AcAl, we titrated the remaining CO or other carbon species on the surface by imping O_2 via the molecular beam at 475 K (as we did during the sample preparation step) in order to conduct other experiments. We also used reflection adsorption infrared spectroscopy (RAIRS) to characterize the remaining molecular species on the Pd−Au surfaces during the desorption and oxidation of the AcAl. All IR spectra were averaged from 512 scans with a resolution of 4 cm^{-1}.

Density Functional Theory (DFT) Calculations. We performed spin-polarized DFT calculations with the Vienna ab initio simulation package.[37] The projector augmented wave framework was employed to treat interactions between the core and valence electrons.[38] Electronic exchange and correlation were described with the revised-Perdew−Burke−Ernzerhof (RPBE) functional.[39] The cutoff energy of the plane wave basis was set to 400 eV, and the Brillouin zone was sampled at 2 × 2 × 1 with the Monkhorst−Pack scheme.[40] The convergence criteria for the electronic structure and geometry were set to 10^{-5} eV and 0.01 eV·$Å^{-1}$, respectively.

The Au slabs used in this study supported different size Pd ensembles in the surface layer. These slabs were constructed with a 5 × 5 supercell containing 4 atomic layers with the bottom 2 layers fixed in their bulk positions. Different numbers of Pd atoms (2, 3, 4, 7, and 25 atoms) of the ensemble were considered to study the effect of the Pd ensemble on adsorption of each intermediate during the AcAl oxidation reaction. These structures are shown in Figure S8. Each slab is separated by a 10 Å vacuum gap in the z-direction to avoid self-interaction.

RESULTS AND DISCUSSION

Since our samples have been annealed at 500 K after the initial deposition of Pd onto Au(111) at 77 K, which causes Pd atoms to diffuse into the Au lattice, the temperature-programmed desorption (TPD) of H_2 was conducted on both 2.0 and 3.0 ML Pd deposited surfaces to quantify the fraction of Pd atoms remaining on the surface after annealing, identified as 0.45 Pd/

DOI: 10.1021/acscatal.9b00079
ACS Catal. 2019, 9, 4360−4368

0.55 Au and 0.8 Pd/0.2 Au, respectively. As previously verified,[21,22] H_2 molecules can be dissociatively adsorbed on the Pd−Au surface. Hydrogen adatoms located at Pd−Au interfaces (or discontinuous and small Pd ensembles) recombinatively desorb between 150 and 300 K, which is higher than the desorption temperature of H_2 from the pure Au(111) surface (100 K − 150 K)[28] and lower than pure Pd surfaces (>300 K).[29,30] When the Pd coverage is increased to have Pd(111)-like islands (or continuous and sufficiently large Pd ensembles to have pure Pd-like character), the recombinative desorption of H_2 can also occur above 300 K, similar to pure Pd surfaces.[17,19,21,27] As shown in Figure 1, we

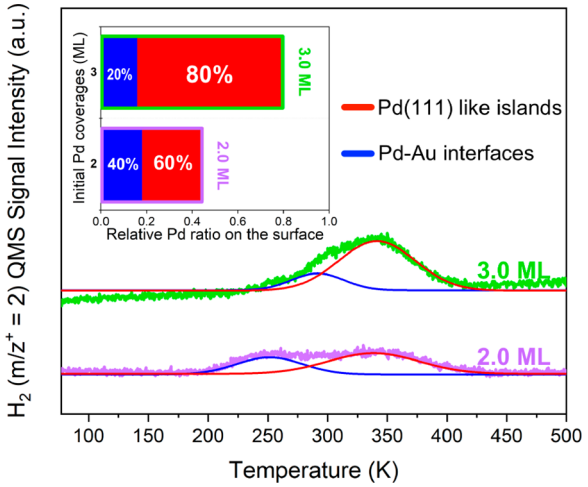

Figure 1. Temperature-programmed desorption (TPD) of H_2 on Pd−Au surfaces. H_2 molecules were impinged at 77 K via a molecular beam on a 2.0 ML Pd initially deposited surface (purple) and 3.0 ML Pd initially deposited surface (green) until the samples were saturated. The saturated samples were heated to 500 K by 1 K/s. Each spectrum is deconvoluted to indicate Pd−Au interface sites (blue) and Pd(111)-like island sites (red). The inset quantifies the relative coverages of the Pd−Au interface sites. and the Pd(111)-like island sites on the 2.0 and 3.0 ML Pd deposited surfaces.

performed a peak deconvolution of the H_2-TPD spectra for which the blue trace represents H_2 desorbing from the Pd−Au interface sites and the red trace indicates H_2 desorption from the Pd(111)-like islands. Based upon the deconvoluted peak areas, the 2.0 ML Pd deposited surface is composed of 40% Pd−Au interface sites and 60% Pd(111)-like islands. On the 3.0 ML Pd deposited surface, the H_2 TPD peak due to the Pd−Au interface sites decreases in magnitude and is shifted to higher temperatures (compared to the 2.0 ML case) showing 20% Pd−Au interface sites and 80% Pd(111)-like island sites. The relative fraction of surface Pd atoms is estimated to be 0.45 for the 2.0 ML case and 0.8 for the 3.0 ML case, determined by comparing each of their H_2-TPD spectra to the spectrum for a 6.0 ML Pd deposited surface (Figure S1) which is fully covered with Pd atoms on its top layer (even after annealing). All of these analyses confirm that the 3.0 ML Pd deposited surface has a stronger Pd-like character than the 2.0 ML case; later we will describe how the surface composition affects the interaction between acetaldehyde (CH_3CHO, AcAl) molecules and oxygen adatoms.

For a better understanding of AcAl surface chemistry, we conducted TPD tests of various coverages of AcAl on the O-free and atomic O-precovered Pd−Au surfaces (Pd: 2.0 ML), where we found that the AcAl molecules are more stabilized on the O-precovered Pd−Au surface and selectively oxidized to acetic acid. In these TPD measurements, we deposited various quantities of AcAl molecules on the Pd−Au surface at 77 K via a molecular beam and then heated the surface to 500 K (at or below which the surface composition is stable). As shown in Figure 2, molecular AcAl desorption (m/z^+ = 29) begins at

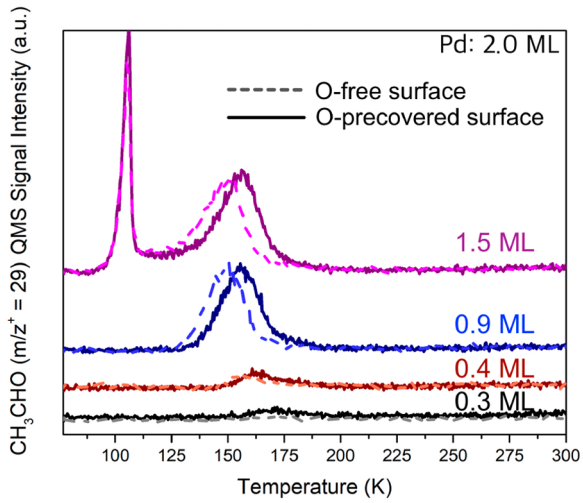

Figure 2. TPD of AcAl on the 2.0 ML Pd deposited surface. Different coverages of the AcAl were impinged via a molecular beam at 77 K, and then they were heated to 500 K by 1 K/s. No desorption features were observed above 200 K. The solid lines indicate AcAl desorption from the oxygen-precovered Pd−Au surface, and the dashed lines describe the AcAl desorption from the oxygen-free Pd−Au surface.

slightly higher temperatures on the O-precovered Pd−Au surface (solid lines) compared with the oxygen-free Pd−Au surface (dashed lines), and no desorption features are observed above 200 K for either surface. Specifically, the oxygen-free surface does not show a molecular desorption feature for 0.3 ML AcAl, but it is observed on the O-precovered surface at ∼175 K. This is an indication that all the AcAl molecules dissociate on the oxygen-free Pd−Au surface (the products of dissociation are displayed in Figure S2) but total dissociation is prevented on the O-precovered surface, a point that will be discussed more fully in the following section. When the AcAl coverage is at 0.4 ML, the oxygen-free surface also starts to show molecular desorption of AcAl with a small peak at 155 K; nevertheless, it does not continue above 175 K. At a coverage of 0.9 ML, the AcAl desorption from the oxygen-free surface begins at 125 K and ends at 175 K with a peak at 150 K, which is a slightly lower temperature than for that on the pure Pd surface (∼160 K).[41] The intensity of the AcAl desorption peak at 150 K is a maximum at a coverage of 0.9 ML AcAl. This can be verified via comparison with the 1.5 ML AcAl adsorbed surface (as shown in Figure S3) which fully covers the surface (i.e., 1 ML) with AcAl and also shows some multilayer desorption of AcAl at 110 K. The desorption spectrum of 0.9 ML AcAl on the O-precovered surface is from 130 to 200 K forming a peak at 160 K, where the overall desorption spectrum is shifted to a slightly higher temperature range compared with the oxygen-free surface. This suggests that the interactions between the AcAl molecules and the surface oxygen adatoms stabilize the AcAl molecules on the Pd − Au surface (which has also been observed on the pure Pd surface[32]). 1.5 ML of AcAl on the O-precovered surface also

DOI: 10.1021/acscatal.9b00079
ACS Catal. 2019, 9, 4360−4368

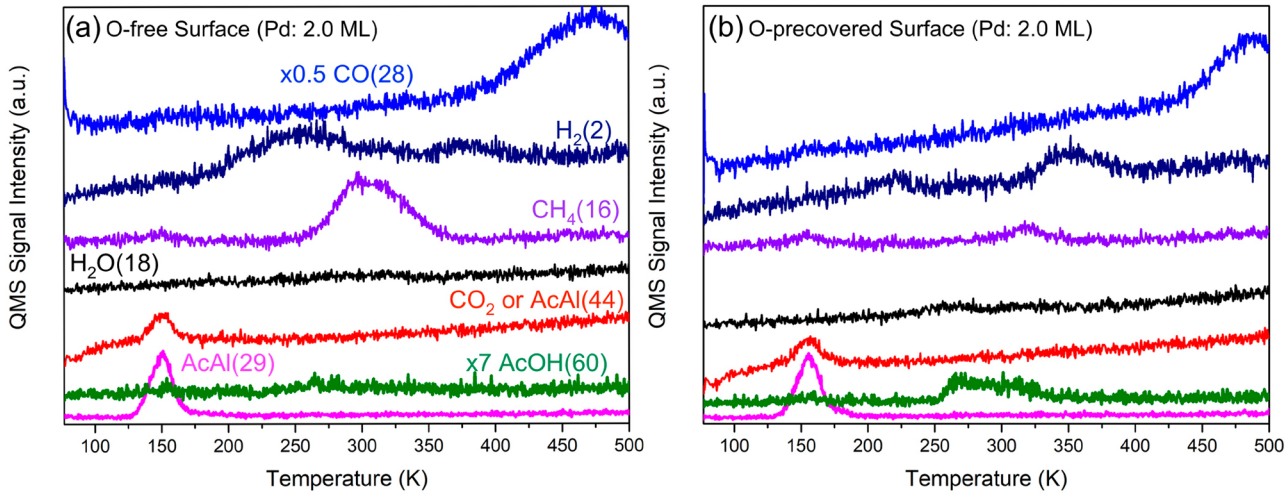

Figure 3. Detailed product analysis during the desorption of 0.9 ML AcAl adsorbed on (a) the O-free Pd−Au surface (Pd: 2.0 ML) and (b) the O-precovered Pd−Au surface (Pd: 2.0 ML). The 0.9 ML AcAl was impinged on the samples at 77 K via the molecular beam, and then the AcAl covered surfaces were heated to 500 K by 1 K/s with observing CO (m/z^+ = 28, blue), H_2 (m/z^+ = 2, dark blue), CH_4 (m/z^+ = 16, mauve), CO_2 or AcAl (m/z^+ = 44, red), AcOH (m/z^+ = 60, green), and AcAl (m/z^+ = 29, magenta). To include all of those spectra in the same scale, the intensity of m/z^+ = 60 is increased by a factor of 7, and the intensity of m/z^+ = 28 is decreased by half.

shows a multilayer desorption peak at 110 K, as with the O-free surface.

On the basis of the results above, we conducted a detailed product analysis during the TPD of AcAl on both oxygen-covered and oxygen-free Au−Pd (2.0 ML Pd) surfaces. In brief, we have discovered that the AcAl molecules are decomposed on the O-free surface, but they are selectively oxidized to AcOH near room temperature on the O-precovered surface. From previous studies on pure Pd, it has been found that residual AcAl molecules remaining after molecular AcAl desorption are fully decomposed to generate H_2 (~300 K), CH_4 (~290 K), and CO (~475 K).[41,42] AcAl decomposition also mainly occurs on the oxygen-free Pd−Au surface (Pd: 2.0 ML). In the TPD spectra for 0.9 ML AcAl on the oxygen-free Pd−Au surface (Figure 3a), H_2 desorption takes place from 175 to 400 K, immediately following the desorption of the molecularly adsorbed monolayer of AcAl. The initiation of H_2 desorption from the oxygen-free Au−Pd (2.0 ML) surface is lower than that from pure Pd surfaces, since the Pd−Au interfaces are the sites for the H_2 desorption from 150 to 300 K, and the Pd(111)-like islands evolve H_2 desorption from 300 to 400 K, as with pure Pd surfaces. The desorption of CH_4 is observed from 250 to 375 K, which is evidence of C−C bond dissociation, and this temperature range corresponds to CH_4 desorption subsequent to AcAl decomposition on pure Pd surfaces.[41,42] After CH_4 desorption begins, the intensity of desorbing H_2 molecules decreases. This observation indicates that the CH_3* fragments from AcAl recombine with H adatoms and leave the surface as CH_4 (CH_3*+ H*), which diminishes the H_2 desorption intensity during CH_4 generation. The remaining C−O fragments on the surface desorb from the surface as CO molecules above 400 K.

On the O-precovered 2.0 ML Pd deposited surface (Figure 3b), the AcAl chemistry is different from that of the oxygen-free Pd−Au surface, and as mentioned earlier, a large increase in the selectivity to production of acetic acid is observed. According to a previous study regarding the O-precovered Pd (pure) surface, oxygen adatoms fully oxidize the AcAl molecules to form H_2O (~300 and ~400 K), CO_2 and AcOH (~400 K), and CO from 450 K.[32] However, we have recently discovered that oxygen adatoms on the Pd−Au surfaces have higher reactivity at relatively low temperatures (especially below 200 K) compared to pure Pd surfaces.[19] Thus, the AcAl molecules can be more selectively oxidized to the acetate and desorb from the surface as AcOH before the decarboxylation of the acetate on the surface occurs. As shown in Figure 3b, when 0.9 ML of AcAl is adsorbed on the O-precovered surface (which is prepared by exposing the Pd−Au surface to O_2 at 300 K[19]) the amount of H_2 and CH_4 generated from the dissociation of AcAl largely decreases during the production of AcOH from 250 to 340 K. Specifically, the H_2 desorption peak is no longer broad and continuous as on the oxygen-free Pd−Au surface; instead there are two desorption features, one before the generation of AcOH, from 200 to 250 K, and the other after most of the AcOH generation is complete, from 325 to 400 K. These results indicate that H atoms are still deprotonated from adsorbed AcAl molecules and are closely related to the formation of AcOH because H_2 desorption terminates during AcOH generation. The desorption intensity of CH_4 (300 K - 325 K) is less than for the oxygen-free Pd−Au case, and the CO generation starts from 450 K, which is higher than for the oxygen-free case (from 400 K) and indicates a lower amount of CO on the oxygen-precovered surface.[43,44] Thus, the O adatoms on the Pd−Au surface both prevent the AcAl molecules from being dissociated and contribute to the formation of AcOH. Since we do not observe the production of CO_2 and H_2O, which is key evidence for the full oxidation of AcAl, it is likely that most of the oxygen adatoms are used to generate AcOH. The AcOH production and desorption temperature is the same as the desorption temperature of AcOH molecularly adsorbed on this Pd−Au surface suggesting a desorption-limited process. The production of AcOH via the oxidation of 0.9 ML of AcAl is estimated to be ~0.3 ML AcOH based on the experiment illustrated in Figure S4 which involves an exposure of 0.3 ML AcOH and its molecular desorption from the surface between 240 to 340 K which gives the same integrated area. Therefore, the AcAl can be selectively oxidized to AcOH on the 2.0 ML Pd deposited surface without generating other oxidized products during the AcOH production, such as CO_2 and

DOI: 10.1021/acscatal.9b00079
ACS Catal. 2019, 9, 4360−4368

H_2O, which have been observed on the pure Pd(111) surface.[32]

For a detailed understanding of the dependence of the production of AcOH on the AcAl coverage, we also analyzed the relative amount of generated H_2 (from C−H bond dissociation), CH_4 (from C−C bond dissociation), and AcOH as shown in Figure 4. (The TPD spectra for 0.3 and 1.5 ML AcAl are shown in Figure S5.) Since the surface is fully saturated with AcAl on a 1.5 ML AcAl covered surface, it shows about 5%, 7.5%, and 6.5% more production of CH_4, H_2, and AcOH, respectively, compared to a 0.9 ML AcAl covered surface, which indicates that 0.9 ML of AcAl molecules react with most of the precovered oxygen adatoms to make AcOH on the 2.0 ML Pd deposited Au (111) surface. The 0.3 ML AcAl covered surface still shows ∼55% of the AcOH production in comparison to the 1.5 ML AcAl case, but the generation of CH_4 and H_2 molecules can be no greater than 5%, as the features at the temperatures over which these molecules desorb have a low signal-to-noise ratio. These results mean that H_2 and CH_4 generation from the 0.9 or 1.5 ML AcAl cases are primarily a result of the overabundance of AcAl molecules which do not interact with the surface oxygen atoms. This again confirms that the oxygen adatoms are the principal contributor to oxidation of AcAl to AcOH and that selectivity toward AcOH can be enhanced when the appropriate coverage of AcAl is provided to the O-precovered Pd−Au surface.

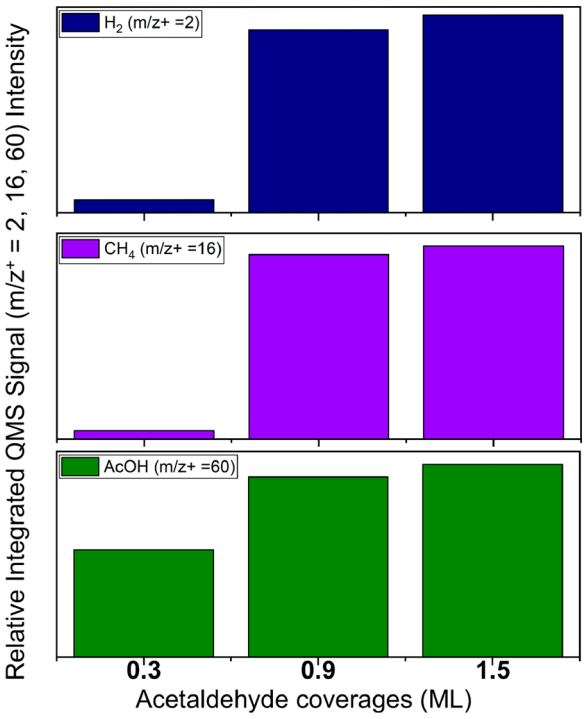

Figure 4. Relative integrated QMS signal intensities of H_2 ($m/z^+ = 2$), CH_4 ($m/z^+ = 16$), and AcOH ($m/z^+ = 60$) generated during the TPD of 0.3, 0.9, and 1.5 ML AcAl on the O-precovered Pd−Au (Pd: 2.0 ML) surface.

After observing the selective oxidation of AcAl to AcOH on the oxygen precovered surface from the TPD measurements, we performed reflective-absorption infrared spectroscopy (RAIRS) measurements to confirm the formation of acetate via the interaction of oxygen adatoms and adsorbed acetaldehyde molecules, which is additional evidence for the production of AcOH, as previously determined.[32,33,45−47] As shown in Figure 5, we focus on the range from 1300 to 2000 cm^{-1}, in which the carbonyl groups of the adsorbed species can be identified, since we want to compare the ν(CO) stretch from the adsorbed acetaldehyde to the ν(CO) stretch from acetate formation. At 160 K, AcAl molecules on the oxygen-free Pd−Au surface (Pd: 2.0 ML) in Figure 5a have two different adsorbed configurations: η^2(C,O)-acetaldehyde as identified by ν(CO) at ∼1400 cm^{-1} and η^1(C)-acetyl as identified by ν(CO) at ∼1600 cm^{-1} (via the deprotonation of

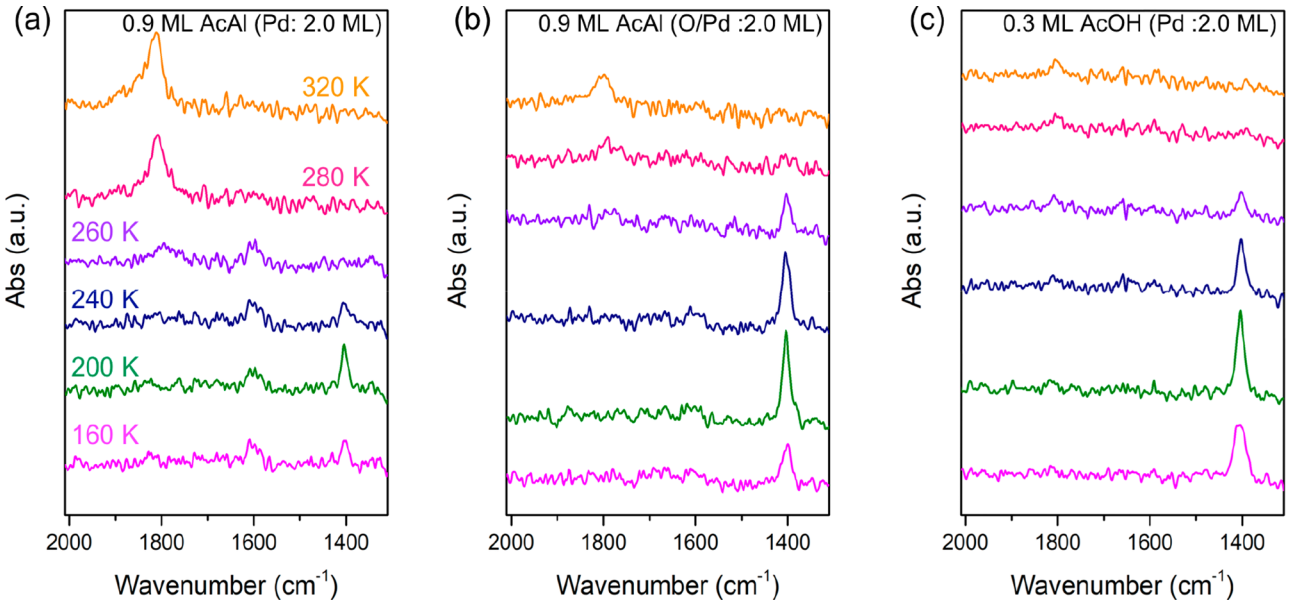

Figure 5. Reflective-adsorption infrared spectroscopy (RAIRS) spectra of (a) 0.9 ML AcAl on the oxygen-free Pd−Au surface (Pd: 2.0 ML), (b) 0.9 ML of AcAl on the oxygen-precovered Pd−Au surface (Pd: 2.0 ML), and (c) 0.3 ML AcOH on the oxygen-free Pd−Au surface (Pd: 2.0 ML). All gas molecules were directed on the samples at 77 K via the molecular beam, and then the samples were heated and held at 160, 200, 240, 260, 280, and 320 K for the IR spectroscopy. The *y*-axis of all of IR spectra under the same scale.

DOI: 10.1021/acscatal.9b00079
ACS Catal. 2019, 9, 4360−4368

AcAl); these assignments correspond to previous observations on pure Pd surfaces.[41,48] After the desorption of most of the AcAl molecules (at 200 K), the intensity of the η^2-acetaldehyde peak increases because some of the weakly bound or η^1-coordinated AcAl molecules are converted to the η^2(C,O) configuration while heating the surface, but this η^2-acetaldehyde peak begins to decrease above 240 K. (These changes in the η^2(C,O)-acetaldehyde peak are consistent with a previous study on the pure Pd(111) surface.[48]) When the temperature reaches 260 K, the η^2-acetaldehyde peak finally disappears; however, the η^1-acetyl peak still exists on the surface and becomes slightly larger and broader than when it was annealed to 200 K. A small and broad peak at ~1805 cm^{-1} begins to be observed from 260 K, and this peak is likely from carbonyl species via the decomposition of the AcAl molecules on Pd ensembles. This feature continuously grows larger and sharper at higher temperatures with a peak at ~1815 cm^{-1}, corresponding to CO via the decomposition of the AcAl as previously detected on pure Pd surfaces.[41,48] This transition indicates C−C bond dissociation, in which the η^1-acetyl peak also fades out during this process. All of these results are not only similar to the previous observations regarding the decomposition of AcAl on pure Pd surfaces[41,48] but also agree with our observations from TPD measurements.

For the case of the O-precovered surface (Pd coverage is still 2.0 ML), the IR spectrum of 0.9 ML AcAl in Figure 5b generally shows different vibrational behavior compared to the oxygen-free surface. At 160 K, Figure 5b shows a more intense peak at ~1400 cm^{-1} compared with the peak at the same wavenumber in Figure 5a (the AcAl on the oxygen-free surface) via the formation of η^2-acetaldehyde. Although we can also see a very weak signal from η^1-acetyl at ~1600 cm^{-1} in Figure 5b from 160 to 260 K, it is not as indicative as in Figure 5a and it is also hard to distinguish the peak from the background noise. Based on these differences in molecular behavior, we can expect the peak at ~1400 cm^{-1} in Figure 5b to be due to η^2(O,O)-acetate since AcOH generation was detected on this surface. This assignment is also supported by the detection of a ν(CO) peak near 1400 cm^{-1} by η^2-acetate as reported in previous studies regarding acetaldehyde oxidation on Pd(111)[32] and AcOH adsorption and desorption from Pd(111),[33,45] Au−Pd(100),[46] and Au−Pd(111)[47] surfaces. This peak is highest at 200 K and starts to diminish at 240 K, which is near the temperature at which the initial production of AcOH is observed. At 280 K, a weak peak at ~1800 cm^{-1} is observed, and it grows slightly larger at 320 K but is still much less intense than for the oxygen-free surface case. This peak can be attributed to decomposed CO species such as on the oxygen-free surface, but these temperatures are still in the range of AcOH production, so the peak at 1800 cm^{-1} could also possibly be formed by physisorbed AcOH monomer based on previous observations, which has ν(CO) positioned at ~1799 cm^{-1}.[47] To compare these results with the AcOH adsorbed on the oxygen-free Pd−Au surface, we measured the IR spectrum of 0.3 ML AcOH adsorbed at 77 K on the oxygen-free Pd−Au (Pd: 2.0 ML) surface. Figure 5c shows similar IR spectra to the case of AcAl coadsorbed on the O-precovered surface for all tested temperatures. Specifically, at 160 K, there is one strong peak near 1400 cm^{-1}, which is the ν(CO) feature for η^2-acetate formed by the deprotonation of AcOH.[33,45−47] With increasing temperatures, the η^2-acetate peak becomes larger at 200 K, but starts to decrease from 240 K onward. At 280 K the η^2-acetate peak disappears but there is a weak peak at ~1800 cm^{-1}, which grows slightly larger at 320 K. These measured vibrational features for a 0.3 ML coverage of AcOH on the oxygen-free surface are analogous to that obtained with 0.9 ML AcAl on the O-precovered surface. This confirms the formation of acetate via the interaction between AcAl and oxygen adatoms. Furthermore, the acetate species formed on this surface can desorb primarily as AcOH instead of undergoing decarboxylation and forming other products as observed on the O-free 2.0 ML Pd deposited surface in Figure 3a.

As shown in Figure 6, when the initial Pd coverage is increased to 3.0 ML, the AcAl molecules can be fully oxidized

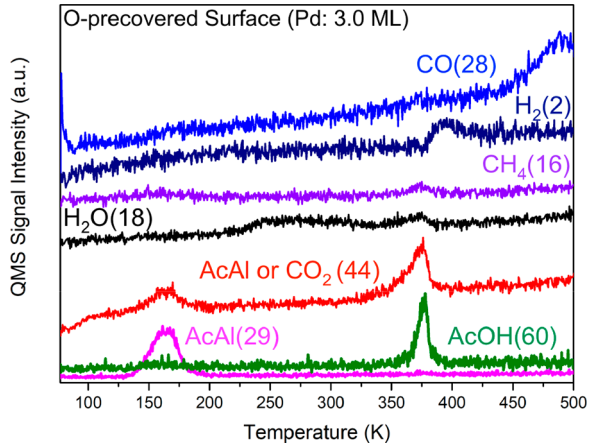

Figure 6. TPD of 0.9 ML AcAl adsorbed on the O-precovered Pd−Au surface (Pd: 3.0 ML). The 0.9 ML AcAl was directed on the surface at 77 K via the molecular beam and then heated to 500 K by 1 K/s with observing CO (m/z^+ = 28, blue), H_2 (m/z^+ = 2, dark blue), CH_4 (m/z^+ = 16, purple), CO_2 or AcAl (m/z^+ = 44, red), AcOH (m/z^+ = 60, green), and AcAl (m/z^+ = 29, magenta). To include all those spectra in the same scale, the intensity of m/z^+ = 60 is increased by a factor of 7, and the intensity of m/z^+ = 28 is decreased by half.

to CO_2 and H_2O at ~375 K while also generating H_2, CH_4, AcOH, and CO, similar to results from pure Pd surfaces. With an increased Pd coverage, there are more Pd-(111) like islands, as verified from the H_2 TPD in Figure 1, leading to a stronger Pd character for the surface. On the oxygen-free 3.0 ML Pd deposited surface, thus, there is less molecular desorption of AcAl, which is 60% as compared to the 2.0 ML Pd deposited surface, so the production of CH_4, H_2, and CO from decomposing AcAl is increased, as shown in Figure S6. These results indicate stronger interactions between the surface and adsorbed AcAl molecules as with pure Pd surfaces.[41] Moreover, more oxygen adatoms can be adsorbed onto the 3.0 ML Pd deposited surface because of the higher Pd coverage, which is about 2.6 times more than the 2.0 ML case, observed via the titration of O adatoms using CO at 400 K in our previous study.[19] However, we have also found that the stronger Pd character in the 3.0 ML case causes the oxygen adatoms to be more strongly bound on the surface and become less reactive at relatively low temperatures compared to the 2.0 ML case.[19] Thus, the 0.9 ML AcAl molecules on the O-precovered surface (Pd: 3.0 ML) in Figure 6 have stronger interactions with the surface itself and also react with oxygen adatoms at higher temperatures in comparison with the 2.0 ML Pd case discussed previously. Specifically, the production of AcOH is observed above 350 K and forms a peak at 375 K, which accompanies the generation of CO_2, H_2O, and CH_4. H_2

DOI: 10.1021/acscatal.9b00079
ACS Catal. 2019, 9, 4360−4368

also evolves from this surface starting at 375 K, which is quite different from the 2.0 ML case (as shown in Figure 3b) since it only generates AcOH without other oxidized species (e.g., H_2O and CO_2). While the m/z^+ = 44 signal can be due to either AcAl or CO_2, we notice that its lower temperature peak is coupled with a m/z^+ = 29 signal, and its higher temperature peak does not have a corresponding m/z^+ = 29 signal, indicating that the lower temperature m/z^+ = 44 peak is caused by AcAl desorption, and the higher temperature peak is generated via CO_2 production. The oxidized species, AcOH, H_2O, and CO_2, are evidence of the decarboxylation of acetate on the surface, which is known to be initiated by dissociating C−H bonds of the acetate species on the surface. This chemistry has also been observed in previous studies regarding the oxidation of AcAl on Pd(111)[32] and the desorption of AcOH on Pd(100)[34] and Pd(111)[45]. Note that in Figure 6 there are two desorption features for H_2O, one of which is from 225 to 330 K while the other is from 330 to 380 K. The lower temperature feature is mainly due to extra oxygen adatoms which scavenge the deprotonated hydrogen atoms on the surface instead of interacting with adsorbed AcAl molecules.[32] The higher temperature water desorption feature is generated during the decarboxylation of the acetate which also generates CO_2 and AcOH. The lower H_2O desorption feature indicates that the H atoms are still deprotonated from the AcAl molecules by forming the acetate species as with the 2.0 ML case, but there is no desorption feature for the AcOH because the formed acetate species on this surface do not recombine with the H adatoms. The less reactive acetate species seem to be decarboxylated from 350 K onward leading to the production of AcOH, H_2O, CO_2, CH_4, and H_2. Although there are some differences in the intensity of the desorbing molecules, the lower (0.3 ML) and higher (1.5 ML) AcAl coverages also show the production of AcOH, H_2O, and CO_2 simultaneously as shown in Figure S7, which means the decarboxylation occurs on this surface independent of the coverage of AcAl. Once again, these observations are similar to previous studies conducted on pure Pd surfaces.[32] Thus, the increased Pd coverage (and hence size of the Pd ensembles) allows the AcAl molecules to be more easily dissociated and less selectively oxidized to AcOH while also generating CO_2 and H_2O, which does not occur on the 2.0 ML case. These results can be understood via DFT calculations of AcAl oxidation at the Pd ensembles on the Au surface.

With our DFT calculations, we aimed to determine the general size effect of Pd ensembles on the adsorption and reaction of AcAl molecules employing a range from 2 Pd atoms to 25 Pd atoms (which covers the whole Au slab as one ML). We subdivide the catalytic oxidation of AcAl into its component steps to understand the chemistry on the Pd−Au surface, where various intermediates are adopted from the experimental TPD analysis to get the most feasible reaction pathways. As shown in Figure 7, the first step involves introducing atomic oxygen onto the surface. The oxygen adatom does not spill over to pure Au sites and is more stable on larger Pd ensembles, as also shown in previous studies.[19] When an AcAl molecule is subsequently adsorbed on the surface in the second step, there are two possible reaction pathways with adsorbed atomic oxygen. In the energetically favorable pathway, a hydrogen atom deprotonates from the AcAl and then the deprotonated AcAl molecule reacts with an oxygen adatom to form a surface bound acetate (CH_3COO*), where the deprotonated H atoms do not spill over to pure Au

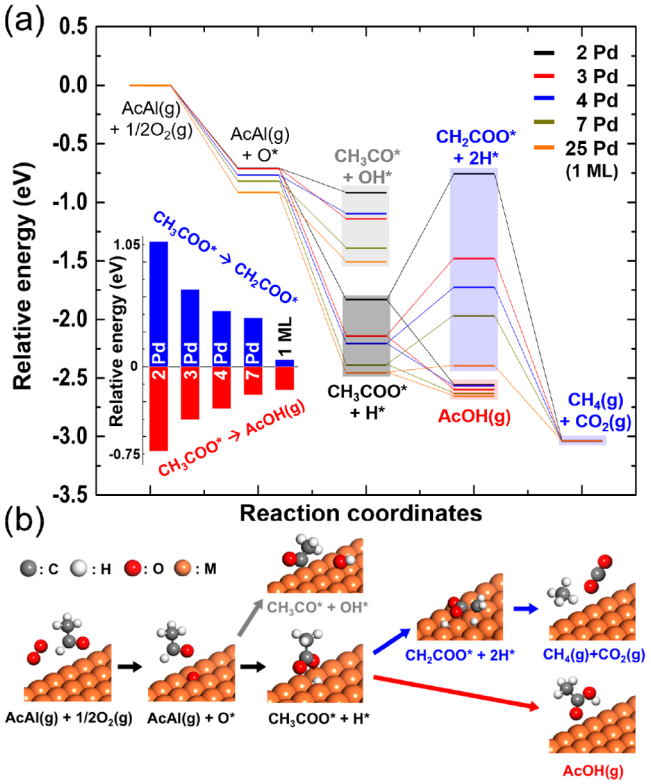

Figure 7. (a) Energy diagram for the catalytic oxidation of AcAl to AcOH or CH_4+CO_2 as a function of Pd ensemble size: 2Pd, 3Pd, 4Pd, 7Pd, and 25Pd (1 ML). (b) The reaction pathways that we consider for AcAl oxidation.

sites but stay on the Pd(111)-like islands as experimentally verified from the H_2 desorption temperatures in Figures 1 and 3. A less favorable pathway has the oxygen adatom scavenging the deprotonated hydrogen from AcAl, which leads to the formation of a hydroxyl (OH*) and an acetyl (CH_3CO*) on the surface. Acetate formation is about 1 eV favorable as compared to acetyl and hydroxyl formation on all surfaces tested, and the acetate species are more stable on higher Pd coverages as shown in Figure 7a. Specifically, the acetate formation is more energetically favorable on the atop sites of the interior of Pd atoms than on the Pd−Au interfaces or on the pure Au sites as shown in Figure S9. We have also found (in Figure 5) that the vibrational frequency of the η^2(O,O)-acetate (~1400 cm^{-1}) on the 2.0 ML Pd deposited surface is close to previously studied values on pure Pd surfaces.[32,46] Moreover, the acetate with a deprotonated hydrogen formed on the 2 or 3Pd atoms is less stable than on the 7Pd atoms as indicated in Figure 7a (−1.83 eV on 2Pd, −2.14 eV on 3Pd, and −2.37 eV on 7Pd) because the acetate and deprotonated hydrogen cannot simultaneously occupy the most stable adsorption sites (e.g., the interior of Pd atoms) on the relatively smaller Pd ensembles. In the third step, the acetate species on each surface has two possible reaction paths: initiation of decarboxylation (blue path) and the formation of AcOH (red path). As shown in Figure 7b (blue arrows) decarboxylation is initiated by dissociation of the β−C-H acetate bond, as has been observed in previous studies.[32−34,45] This process is not energetically favorable; the acetate molecule requires additional energy to surmount this step. The energy difference between the acetate and the initial decarboxylation step (CH_2COO*+2H*), as indicated by the

DOI: 10.1021/acscatal.9b00079
ACS Catal. 2019, 9, 4360−4368

blue bar graph in the inset of Figure 7a, is highly dependent on Pd ensemble size, where 2 Pd atoms (black) show a 1.08 eV energy difference and 25 Pd atoms (1 ML Pd, orange) shows only 0.06 eV. Although AcOH formation (red path in Figure 7a,b) is an energetically favorable path for all Pd coverages, its relative stability compared to acetate continuously decreases, as indicated by the red bar graph in the inset of Figure 7a. Thus, the energy differences between acetate and the initial decarboxylation step are reduced with Pd coverage and become very small at 1 ML, indicating that it is feasible for the acetate species to overcome the initial decarboxylation step and become fully decarboxylated as CH_4 and CO_2 on highly Pd-covered surfaces. This analysis implies that higher Pd coverages lead to a lower selectivity toward AcOH in the oxidation of AcAl. These calculations support the experimental observations described above, in which AcOH production is less selective on surfaces with more Pd (3.0 ML), and more selective on surfaces with less Pd (2.0 ML).

Based on these experimental and computational results we can say that the selectivity toward AcOH formation is highly dependent on the Pd ensemble size. As described in Figure 7b (blue arrows), acetate is tilted on the surface to initiate decarboxylation by dissociating the β−C−H bond. If the Pd ensembles are small enough, the tilted acetate species will spill over to the Pd−Au interface or pure Au sites, which are less reactive compared to the Pd(111)-like islands. Thus, the acetate species on the smaller Pd ensembles are unlikely to undergo decarboxylation and instead desorb as AcOH below the initiation temperature for decarboxylation.

CONCLUSION

We have investigated the selective oxidation of acetaldehyde (AcAl) to acetic acid (AcOH) on Pd−Au(111) heterogeneous model catalysts. For testing AcAl oxidation, we used two different Pd coverages on the Au(111) surface: 2.0 and 3.0 ML (0.45 and 0.8 relative amount of Pd atoms on the top surface respectively after annealing to 500 K). On the 2.0 ML Pd deposited surface, the selective production of AcOH from 250 to 340 K was observed during temperature-programmed desorption measurements without generating CO_2 and H_2O. We also detected the formation of acetate species on this surface from 160 to 260 K using RAIRS, which is a representative adsorbed configuration of the AcOH molecule on metal surfaces. We also confirmed that the molecular vibrations caused by coadsorbed oxygen adatoms and AcAl molecules are quite similar to the molecular vibrations of AcOH molecules placed on this surface. However, on a 3.0 ML Pd deposited surface, AcAl molecules were less selectively oxidized to AcOH at higher temperatures (~375 K) and CO_2, H_2O, CH_4, and H_2 were also generated. This is clear evidence for the decarboxylation of the acetate, chemistry which has also been observed on pure Pd surfaces.[32−34,45] DFT calculations show that the relative energy between the acetate state and the initial decarboxylation step is systematically reduced with increasing Pd ensemble size, which leads to facile decarboxylation at higher Pd coverages. This study shows that it is possible to selectively oxidize acetaldehyde to acetic acid near room temperature by controlling the Pd ensemble sizes on a model palladium gold alloy surface.

ASSOCIATED CONTENT

Supporting Information

The Supporting Information is available free of charge on the ACS Publications website at DOI: 10.1021/acscatal.9b00079.

Illustration of Pd−Au(111) surfaces for DFT calculations and results from H_2-TPD spectra on the Pd−Au surfaces, AcAl-TPD spectra on the oxygen-free and oxygen-precovered Pd−Au surfaces, and AcOH-TPD spectra on the 2.0 ML Pd deposited surface (PDF)

AUTHOR INFORMATION

Corresponding Author

*E-mail: mullins@che.utexas.edu.

ORCID

Kihyun Shin: 0000-0002-1748-8773

Graeme Henkelman: 0000-0002-0336-7153

C. Buddie Mullins: 0000-0003-1030-4801

Notes

The authors declare no competing financial interest.

ACKNOWLEDGMENTS

We are thankful for the generous support of the Department of Energy Basic Energy Sciences (Grant DE-SC0018116 (C.B.M.) and Grant DE-SC0010576 (G.H.)) and the Welch Foundation (Grant F-1436 (C.B.M.) and Grant F-1841 (G.H.)). S.H. was partially supported by the Dorothy Banks Fellowship. Computational resources were provided by the Texas Advanced Computing Center and the National Energy Research Scientific Computing Center.

REFERENCES

(1) Pal, P.; Nayak, J. Acetic Acid Production and Purification: Critical Review Towards Process Intensification. *Sep. Purif. Rev.* **2017**, *46*, 44−61.

(2) Sano, K.; Uchida, H.; Wakabayashi, S. A New Process for Acetic Acid Production by Direct Oxidation of Ethylene. *Catal. Surv. Jpn.* **1999**, *3*, 55−60.

(3) Chenier, P. J. *Survey of Industrial Chemistry*; Springer US: Boston, MA, 2002.

(4) Sunley, G. J.; Watson, D. J. High Productivity Methanol Carbonylation Catalysis Using Iridium. *Catal. Today* **2000**, *58*, 293−307.

(5) Han, Y.; Wang, J.; Kumar, D.; Yan, Z.; Goodman, D. A Kinetic Study of Vinyl Acetate Synthesis over Pd-Based Catalysts: Kinetics of Vinyl Acetate Synthesis over Pd−Au/SiO_2 and Pd/SiO2 Catalysts. *J. Catal.* **2005**, *232*, 467−475.

(6) Kumar, D.; Chen, M. S.; Goodman, D. W. Synthesis of Vinyl Acetate on Pd-Based Catalysts. *Catal. Today* **2007**, *123*, 77−85.

(7) Edwards, J. K.; Solsona, B.; N, E. N.; Carley, A. F.; Herzing, A. a.; Kiely, C. J.; Hutchings, G. J. Switching Off Hydrogen Peroxide Hydrogenation in the Direct Synthesis Process. *Science* **2009**, *323*, 1037−1041.

(8) Wilson, N. M.; Priyadarshini, P.; Kunz, S.; Flaherty, D. W. Direct Synthesis of H_2O_2 on Pd and Au_xPd_1 Clusters: Understanding the Effects of Alloying Pd with Au. *J. Catal.* **2018**, *357*, 163−175.

(9) Edwards, J. K.; Hutchings, G. J. Palladium and Gold-Palladium Catalysts for the Direct Synthesis of Hydrogen Peroxide. *Angew. Chem., Int. Ed.* **2008**, *47*, 9192−9198.

(10) Enache, D. I.; Edwards, J. K.; Landon, P.; Solsona-Espriu, B.; Carley, A. F.; Herzing, A. A.; Watanabe, M.; Kiely, C. J.; Knight, D. W.; Hutchings, G. J. Solvent-Free Oxidation of Primary Alcohols to Aldehydes Using Au-Pd/TiO_2 Catalysts. *Science* **2006**, *311*, 362−365.

DOI: 10.1021/acscatal.9b00079
ACS Catal. 2019, 9, 4360−4368

(11) Hou, W.; Dehm, N. A.; Scott, R. W. J. Alcohol Oxidations in Aqueous Solutions Using Au, Pd, and Bimetallic AuPd Nanoparticle Catalysts. *J. Catal.* **2008**, *253*, 22−27.
(12) Chen, Y.; Lim, H.; Tang, Q.; Gao, Y.; Sun, T.; Yan, Q.; Yang, Y. Solvent-Free Aerobic Oxidation of Benzyl Alcohol over Pd Monometallic and Au-Pd Bimetallic Catalysts Supported on SBA-16 Mesoporous Molecular Sieves. *Appl. Catal., A* **2010**, *380*, 55−65.
(13) Scott, R. W. J.; Sivadinarayana, C.; Wilson, O. M.; Yan, Z.; Goodman, D. W.; Crooks, R. M. Titania-Supported PdAu Bimetallic Catalysts Prepared from Dendrimer-Encapsulated Nanoparticle Precursors. *J. Am. Chem. Soc.* **2005**, *127*, 1380−1381.
(14) Xu, J.; White, T.; Li, P.; He, C.; Yu, J.; Yuan, W.; Han, Y.-F. Biphasic Pd−Au Alloy Catalyst for Low-Temperature CO Oxidation. *J. Am. Chem. Soc.* **2010**, *132*, 10398−10406.
(15) Kim, H. Y.; Henkelman, G. CO Adsorption-Driven Surface Segregation of Pd on Au/Pd Bimetallic Surfaces: Role of Defects and Effect on CO Oxidation. *ACS Catal.* **2013**, *3*, 2541−2546.
(16) Chen, M.; Kumar, D.; Yi, C.-W.; Goodman, D. W. The Promotional Effect of Gold in Catalysis by Palladium-Gold. *Science* **2005**, *310*, 291−293.
(17) Yu, W.-Y.; Mullen, G. M.; Flaherty, D. W.; Mullins, C. B. Selective Hydrogen Production from Formic Acid Decomposition on Pd−Au Bimetallic Surfaces. *J. Am. Chem. Soc.* **2014**, *136*, 11070−11078.
(18) Yu, W.-Y.; Zhang, L.; Mullen, G. M.; Henkelman, G.; Mullins, C. B. Oxygen Activation and Reaction on Pd−Au Bimetallic Surfaces. *J. Phys. Chem. C* **2015**, *119*, 11754−11762.
(19) Han, S.; Mullins, C. B. Surface Alloy Composition Controlled O_2 Activation on Pd−Au Bimetallic Model Catalysts. *ACS Catal.* **2018**, *8*, 3641−3649.
(20) Yu, W.-Y.; Mullen, G. M.; Mullins, C. B. Interactions of Hydrogen and Carbon Monoxide on Pd−Au Bimetallic Surfaces. *J. Phys. Chem. C* **2014**, *118*, 2129−2137.
(21) Yu, W.-Y.; Mullen, G. M.; Mullins, C. B. Hydrogen Adsorption and Absorption with Pd−Au Bimetallic Surfaces. *J. Phys. Chem. C* **2013**, *117*, 19535−19543.
(22) Lucci, F. R.; Darby, M. T.; Mattera, M. F. G.; Ivimey, C. J.; Therrien, A. J.; Michaelides, A.; Stamatakis, M.; Sykes, E. C. H. Controlling Hydrogen Activation, Spillover, and Desorption with Pd−Au Single-Atom Alloys. *J. Phys. Chem. Lett.* **2016**, *7*, 480−485.
(23) Gao, F.; Wang, Y.; Goodman, D. W. CO Oxidation over AuPd(100) from Ultrahigh Vacuum to Near-Atmospheric Pressures: The Critical Role of Contiguous Pd Atoms. *J. Am. Chem. Soc.* **2009**, *131*, 5734−5735.
(24) Li, Z.; Gao, F.; Tysoe, W. T. Carbon Monoxide Oxidation over Au/Pd(100) Model Alloy Catalysts †. *J. Phys. Chem. C* **2010**, *114*, 16909−16916.
(25) Gao, F.; Wang, Y.; Cai, Y.; Goodman, D. W. CO Oxidation on Pt-Group Metals from Ultrahigh Vacuum to Near Atmospheric Pressures. 2. Palladium and Platinum. *J. Phys. Chem. C* **2009**, *113*, 174−181.
(26) Han, S.; Evans, E. J.; Mullen, G. M.; Mullins, C. B. H_2O-Improved O_2 Activation on the Pd−Au Bimetallic Surface. *Chem. Commun.* **2017**, *53*, 3990−3993.
(27) Evans, E. J.; Li, H.; Yu, W.-Y.; Mullen, G. M.; Henkelman, G.; Mullins, C. B. Mechanistic Insights on Ethanol Dehydrogenation on Pd−Au Model Catalysts: A Combined Experimental and DFT Study. *Phys. Chem. Chem. Phys.* **2017**, *19*, 30578−30589.
(28) Pan, M.; Flaherty, D. W.; Mullins, C. B. Low-Temperature Hydrogenation of Acetaldehyde to Ethanol on H-Precovered Au(111). *J. Phys. Chem. Lett.* **2011**, *2*, 1363−1367.
(29) Gdowski, G. E.; Felter, T. E.; Stulen, R. H. Effect of Surface Temperature on the Sorption of Hydrogen by Pd(111). *Surf. Sci.* **1987**, *181*, L147−L155.
(30) Okuyama, H.; Siga, W.; Takagi, N.; Nishijima, M.; Aruga, T. Path and Mechanism of Hydrogen Absorption at Pd(100). *Surf. Sci.* **1998**, *401*, 344−354.
(31) Liu, X.; Xu, B.; Haubrich, J.; Madix, R. J.; Friend, C. M. Surface-Mediated Self-Coupling of Ethanol on Gold. *J. Am. Chem. Soc.* **2009**, *131*, 5757−5759.
(32) Davis, J. L.; Barteau, M. A. The Interactions of Oxygen with Aldehydes on the Pd(111) Surface. *Surf. Sci.* **1992**, *268*, 11−24.
(33) Davis, J. L.; Barteau, M. A. Hydrogen Bonding in Carboxylic Acid Adlayers on Pd(111): Evidence for Catemer Formation. *Langmuir* **1989**, *5*, 1299−1309.
(34) Li, Z.; Gao, F.; Tysoe, W. T. Surface Chemistry of Acetic Acid on Clean and Oxygen-Covered Pd(100). *Surf. Sci.* **2008**, *602*, 416−423.
(35) Flaherty, D. W.; Hahn, N. T.; Ferrer, D.; Engstrom, T. R.; Tanaka, P. L.; Mullins, C. B. Growth and Characterization of High Surface Area Titanium Carbide. *J. Phys. Chem. C* **2009**, *113*, 12742−12752.
(36) Koel, B. E.; Sellidj, A.; Paffett, M. T. Ultrathin Films of Pd on Au(111): Evidence for Surface Alloy Formation. *Phys. Rev. B: Condens. Matter Mater. Phys.* **1992**, *46*, 7846−7856.
(37) Kresse, G.; Furthmüller, J. Efficiency of Ab-Initio Total Energy Calculations for Metals and Semiconductors Using a Plane-Wave Basis Set. *Comput. Mater. Sci.* **1996**, *6*, 15−50.
(38) Blöchl, P. E. Projector Augmented-Wave Method. *Phys. Rev. B: Condens. Matter Mater. Phys.* **1994**, *50*, 17953−17979.
(39) Hammer, B.; Hansen, L.; Nørskov, J. Improved Adsorption Energetics within Density-Functional Theory Using Revised Perdew-Burke-Ernzerhof Functionals. *Phys. Rev. B: Condens. Matter Mater. Phys.* **1999**, *59*, 7413−7421.
(40) Monkhorst, H. J.; Pack, J. D. Special Points for Brillouin-Zone Integrations. *Phys. Rev. B* **1976**, *13*, 5188−5192.
(41) Shekhar, R.; Barteau, M. A.; Plank, R. V.; Vohs, J. M. Adsorption and Reaction of Aldehydes on Pd Surfaces. *J. Phys. Chem. B* **1997**, *101*, 7939−7951.
(42) Bowker, M.; Holroyd, R.; Perkins, N.; Bhantoo, J.; Counsell, J.; Carley, A.; Morgan, C. Acetaldehyde Adsorption and Catalytic Decomposition on Pd(110) and the Dissolution of Carbon. *Surf. Sci.* **2007**, *601*, 3651−3660.
(43) Kuhn, W. K.; Szanyi, J.; Goodman, D. W. CO Adsorption on Pd(111): The Effects of Temperature and Pressure. *Surf. Sci.* **1992**, *274*, L611−L618.
(44) Guo, X.; Yates, J. T. Dependence of Effective Desorption Kinetic Parameters on Surface Coverage and Adsorption Temperature: CO on Pd(111). *J. Chem. Phys.* **1989**, *90*, 6761−6766.
(45) Haley, R. D. R.; Tikhov, M. M. S.; Lambert, R. M. The Surface Chemistry of Acetic Acid on Pd{111}. *Catal. Lett.* **2001**, *76*, 125−130.
(46) Li, Z.; Tysoe, W. T. The Adsorption of Acetic Acid on Clean and Oxygen-Covered Au/Pd(100) Alloy Surfaces. *Surf. Sci.* **2012**, *606*, 1934−1941.
(47) Li, Z.; Calaza, F.; Gao, F.; Tysoe, W. T. The Adsorption of Acetic Acid on Au/Pd(111) Alloy Surfaces. *Surf. Sci.* **2007**, *601*, 1351−1357.
(48) Davis, J. L.; Barteau, M. A. Polymerization and Decarbonylation Reactions of Aldehydes on the Pd(11 1) Surface. *J. Am. Chem. Soc.* **1989**, *111*, 1782−1792.

DOI: 10.1021/acscatal.9b00079
ACS Catal. 2019, 9, 4360−4368